ELSEVIER

Journal of Structural Geology 27 (2005) 1644–1657

JOURNAL OF STRUCTURAL GEOLOGY

www.elsevier.com/locate/jsg

Folded onlap geometries: implications for recognition of syn-sedimentary folds

Antonio M. Casas-Sainz[a,*], Ruth Soto-Marín[b], Ángel González[a], Juan José Villalaín[b]

[a]*Departamento de Geología, Universidad de Zaragoza, 50009 Zaragoza, Spain*
[b]*Departamento de Física, Escuela Politécnica Superior, Universidad de Burgos, Avenida de Cantabria s/n, 09006 Burgos, Spain*

Received 28 July 2004; received in revised form 5 May 2005; accepted 15 May 2005
Available online 14 July 2005

Abstract

Growth strata are usually analysed from geological maps, outcrop geometry or seismic sections. Many growth folds have been defined from geological maps, especially in areas where plunging structures allow the syn-tectonic sequence to be displayed at the surface. The geometrical arrangement of these syn-tectonic sequences can also be defined from the relationships between pre-growth and growth strata, as obtained from geological maps. In this paper, from theoretical models and natural examples from the southern Pyrenees, we argue that some cartographic patterns of strata associated with variably plunging folds, traditionally ascribed to syn-tectonic sedimentation with thinning of sedimentary units toward the anticlinal hinge zone, can be explained as completely post-sedimentary folds of sedimentary units lapping onto an inclined bedding surface, and linked to basin margin, or downlap geometries on the basin floor. We conclude that 3-D analysis of syn-tectonic structures, combining data from independent sources (i.e. geological maps and seismic reflection profiles) is essential to determine relationships between sedimentary units and structures.

Keywords: Growth strata; Geometry; Fold; Syn-sedimentary structures; Pyrenees

1. Introduction

Analysis of growth strata is a very important tool for determining the kinematics of folds at shallow crustal levels (Suppe et al., 1992). Geological maps, outcrop views and analysis of seismic reflection profiles help to determine the geometry of growth strata above pre-growth units (see e.g. Vergés et al., 2002, and references therein). In many cases, larger scale structures post-dating folds exhume the pre- and syn-growth sequences, allowing pseudo-3-D analysis of growth structures to be performed (Millán et al., 1994; Poblet et al., 1997).

The outcrop pattern of syn-tectonic strata is often the main tool for defining their relationships with their substratum, especially in areas (such as the southern Pyrenees) where a complete sedimentary record is preserved and the outcrop conditions are good. Thinning of units in the hinge zone of anticlines is usually considered as evidence of coeval fold growth and sedimentation (Millán et al., 1994). The stratigraphic series can then be divided into a pre-growth sequence (with constant thickness) and a syn-growth sequence (with variable thickness) from which the velocity and growing rates of folds can be obtained (Suppe et al., 1992; Millán et al., 1994; Poblet et al., 1997; Storti and Poblet, 1997), provided that rocks of the syn-tectonic sequence can be dated. Unless a significant post-folding palaeotopography is preserved, the 'post-growth' sequence will not show significant changes of thickness related to the hinge zone of folds. Nevertheless, it can be deformed by subsequent re-activation of the same folds, after deposition of the whole sequence (Millán et al., 1994).

In our analysis we have considered that the cartographic pattern of hinge-thinning strata can be achieved either by: (i) coeval folding and sedimentation, with a 'real' thinning of beds belonging to the syn-growth sequence onto the active hinge zone of the anticline, or (ii) by sequential sedimentation and folding, the 'apparent' thinning of the sequence onto the hinge zone due to a combined geometrical effect of onlap (or downlap) of the syn-onlap

* Corresponding author. Tel.: +34 976 762072; fax: +34 976 761106.
E-mail address: acasas@posta.unizar.es (A.M. Casas-Sainz).

0191-8141/$ - see front matter © 2005 Elsevier Ltd. All rights reserved.
doi:10.1016/j.jsg.2005.05.005

sequence onto the top beds of the pre-onlap sequence. Later folding of this sedimentary arrangement in a direction perpendicular or oblique to the pinchout line would lead to a cartographic pattern with the sequence apparently thinning onto the hinge zone (Fig. 1). This means that folding post-dates the hypothetical growth-strata, and can be contemporary with the rotation of the whole structure around a horizontal axis in a direction perpendicular or oblique to folding (Fig. 1). Our aim is to develop this second hypothesis in order to finally establish criteria to distinguish between this model and actual syn-sedimentary folds.

Although the geometry and kinematics proposed may seem an ad-hoc explanation for the geometrical arrangement found in nature, it is important to note that onlap geometries are common at basin margins and that the localisation of deformation runs are usually parallel to

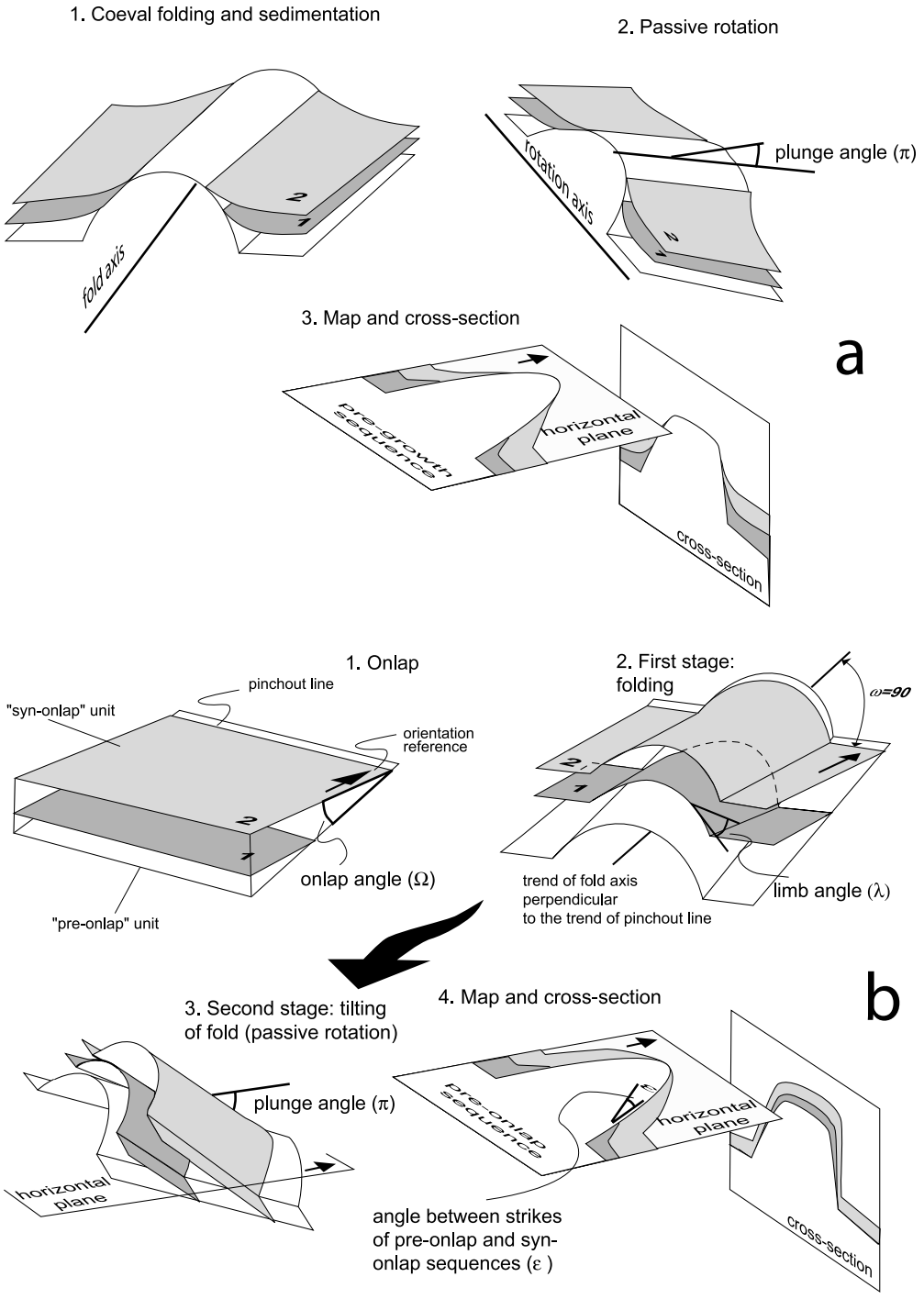

Fig. 1. Sketch showing the geometrical analysis and variables used in this work. (a) Actual growth strata scenario. (b) Model with a folded onlap geometry. See text for explanation.

previous structures on basin margins (Cortés et al., 1999). In marine sediments onlap and downlap geometries are practically ubiquitous within the architectural scheme of depositional sequences (Van Wagoner et al., 1988). In this sense, it is reasonable to expect the kind of structure proposed.

In this paper we illustrate the theoretical analysis of growth strata with a particular kind of growth structure appearing in the southern Pyrenees, in which first-stage folds associated with growth strata were later transported in the hanging wall of thrust sheets.

In many cases the earlier folds overlie footwall ramps of younger thrusts and plunge toward the hinterland, thus allowing the growth of stratigraphic sequences to be analysed in map view. A series of these folds is found in the Sierras Exteriores Aragonesas (Millán et al., 1994), with a northward plunge associated with the Southern Pyrenean frontal thrust. Another series of folds is found in the northern sector of the Cotiella-Bóixols Nappe (Turbón and Egea anticlines; Simó, 1985). In this case, fold axes plunge to the South, as a consequence of the uplift of the Axial Zone of the Pyrenees. We first describe the qualitative and quantitative geometrical models analysed in a general way, and apply it later to the proposed examples. The analysis shown in this paper will probably help to understand some apparent geometrical incompatibilities occurring in growth folds, especially some features displayed in seismic sections (where the 3-D control of geological structures is poor).

2. Geometrical models

2.1. Qualitative description of the geometrical model

We consider as a reference an arrangement with onlap or downlap geometry with pinchout lines in an E–W direction (Fig. 2a and b) and the syn-onlap sequence progressively thinning to the North. Folding creates a flexural fold, oriented in a N–S direction that is then passively rotated about an E–W axis. The resulting cartographic pattern of the previous pinchout geometry will differ depending on the plunge direction (Fig. 2c–f). Units of the syn-onlap sequence will be apparently thickened in the hinge zone of the anticline if the anticline plunges to the South (Fig. 2c), and will be apparently thinned in the hinge zone if the anticline plunges to the North (Fig. 2d–f). If the folding direction is oblique to the pinchout lines of the 'syn-tectonic' unit, the resulting cartographic pattern will show an asymmetric geometry, with the maximum apparent hinge thickening (in the case of southward plunge) or thinning (in the case of northward plunge) displaced with respect to the hinge of the fold in the pre-onlap sequence (Fig. 2g–i). This geometry is very similar to the one obtained from syn-onlap sequences deposited during hinge migration of the early anticline (Millán et al., 1994). An end-member case will appear if the pinchout line is parallel to the fold axis (Fig. 2k). In this case, most parts of the 'syn-onlap' unit crops out only in one of the limbs of the anticline (the southern limb in the example presented).

In the case of downlap geometry (Fig. 2b) the cartographic patterns would be very similar to the onlap, provided that the sequence thins in the same direction, except that: (i) the pre-growth sequence was horizontal before deformation, and (ii) the syn-growth series would not be originally horizontal.

2.2. Quantitative analysis

To describe the models several angles are needed (Figs. 1 and 3), namely: (i) the onlap or downlap angle between the pre-onlap and the syn-onlap series (Ω); (ii) the dip of limbs due to first-stage folding (λ); (iii) the plunge of the fold after tilting (π), consequence of passive rotation around a horizontal axis perpendicular to the axis of the first fold, and (iv) the angle between the trend of the pinchout lines of the lapout (intersection between the planes of the pre-onlap and syn-onlap sequences) and the trend of the first-phase fold (ω). The angle between the strikes of the pre-onlap and the syn-onlap sequences (ε), which gives a clue to the cartographic pattern that will be obtained for each structure, is used in many of the results presented (Figs. 1 and 2). In many of the models presented here, we assume the simplification of considering that the two rotation axes describing this kind of deformation, associated with folding and plunging, respectively, are perpendicular. However, calculations can be easily adapted for different cases including oblique rotation axes, according to the natural examples analysed. Another important assumption is that in our models flexural-slip is considered the main folding mechanism, even if kink-fold geometry is often used to represent the cartographic patterns. Because of the small values of angles involved, and rotation values lower than 90°, the maximum expected changes in the onlap angles due to flexural-slip are about 2° (Ramsay, 1967) when the shear due to flexural-slip is perpendicular to the pinchout lines.

Forward modelling of rotations about two perpendicular axes allows the cartographic patterns resulting from deformation to be obtained (Figs. 2e, f, i and j and 3). The critical variable that determines the cartographic pattern, and thus gives the appearance of growth strata associated with folding, is the angle between the strikes of beds of the pre- and syn-onlap sequences (angle ε in Fig. 1). This angle will be the same in both limbs of the anticline if the pinchout line is perpendicular to the first fold axis (therefore, $\omega = 90°$), and will be different in both limbs of the fold if $\omega \neq 90$. We have considered only two cases, in both of which the two rotation axes are perpendicular, and ω values are 45 and 90°, respectively (Fig. 3c and e). Similar calculations can be made for different values of ω.

In the diagrams presented we applied sequential limb rotation and plunge rotation (two perpendicular axes; Fig. 3). Other conditions with non-perpendicular axes can

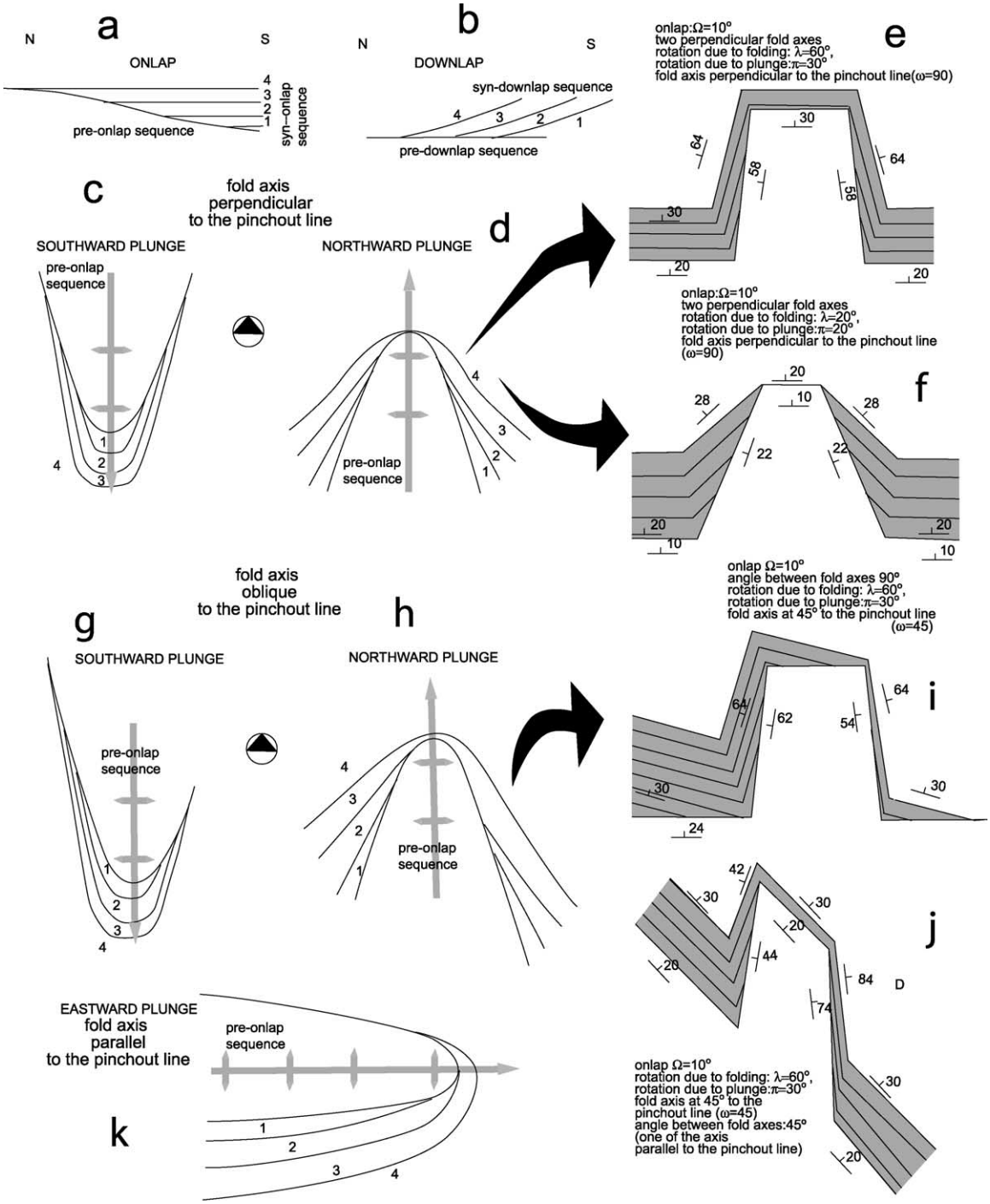

Fig. 2. Sketches showing qualitative and quantitative map patterns of sequences lapping onto the pre-onlap sequence and pre-dating folding (see text for detailed explanation). (a) Geometrical arrangement with onlap geometry used. (b) Arrangement with equivalent downlap geometry. (c) Cartographic pattern of the pre- and syn-onlap sequences of (a) for a southward plunging fold. (d) Cartographic patterns for northward plunging folds. (e) and (f) Cartographic patterns obtained from quantitative analysis and modelling from the diagrams shown in Fig. 4. Parameters shown in each sketch. (g) Cartographic pattern resulting from southward-plunging fold with pinchout lines of the syn-onlap sequence oblique to the fold axis. (h) Cartographic pattern for a northward-plunging fold. (i) Quantitative model (parameters indicated) of the northward-plunging fold and fold axis oblique to the pinchout lines. (j) Cartographic pattern in which the two-fold axes are at 45° and the pinchout lines are parallel to the second axis. (k) Cartographic pattern for the case in which the fold axis is parallel to the pinchout lines (both trending E–W) and the second deformation stage involves an eastward plunge of the anticline.

also be modelled by the same method, according to the equations presented below. It is important to note that rotations are not interchangeable and that the results obtained would not be the same if rotation due to plunging (π) is applied before rotation associated with the fold limb (λ). To simplify, we consider only one of the possibilities,

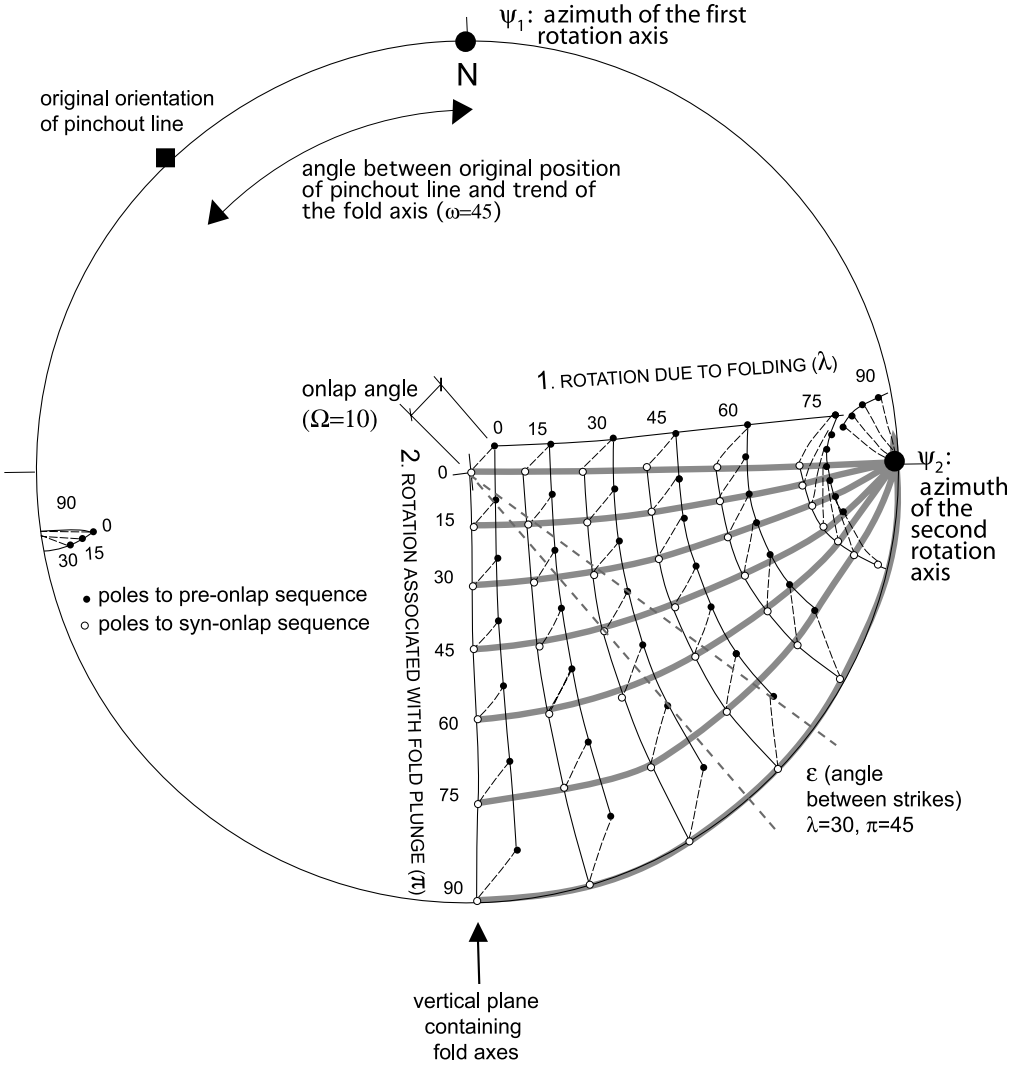

Fig. 3. Stereoplot showing the position of poles to bedding planes of the pre-onlap (considered with a 10°SW dip) and syn-onlap sequences (considered as originally horizontal) according to an onlap angle $\Omega = 10°$, and different dip of fold limbs (λ) and plunge (π), up to 90°. The original pinchout line of the syn-onlap sequence forms an angle of 45° with the first stage fold axis, and shows a NW–SE trend in the stereogram. Poles for the westlimb of a N–S horizontal fold (λ) tilted northward (π), assuming a flexural-slip mechanism. The calculation of the ε angle for the particular case with $\lambda = 30$ and $\pi = 45$.

that is, sequential folding and plunging (Fig. 3), because it seems to fit better with the natural examples analysed in this paper. The same can be easily applied in the reverse order, according to the equations presented below, but the values appearing in the diagrams shown in Fig. 4 would then be different. The relationships used to obtain the diagrams were easily obtained from Euclidean geometrical relationships (Spiegel, 1998) as follows:

A bedding plane can be represented by the unit vector with the dip direction of the bed (always pointing downwards), with its three coordinates:

$$\begin{bmatrix} X \\ Y \\ Z \end{bmatrix} = \begin{bmatrix} \cos\delta \cdot \cos\beta \\ \sin\delta \cdot \cos\beta \\ -\sin\beta \end{bmatrix},$$

where δ is the strike of the bed and β its dip, assuming that the North direction is represented by the y axis (0,1,0) of the coordinate system.

Let ψ_1 be the azimuth of the first rotation axis, $\theta_1 = 90 + \psi_1$, the azimuth perpendicular to this axis (always lower than 360°) and λ be the amount of rotation, then the coordinates of the vector representing the rotated plane can be obtained according to the matrix product (see also Fig. 3):

$$\begin{bmatrix} X' \\ Y' \\ Z' \end{bmatrix} = \begin{bmatrix} \cos\theta_1 & -\sin\theta_1 & 0 \\ \sin\theta_1 & \cos\theta_1 & 0 \\ 0 & 0 & 1 \end{bmatrix} \begin{bmatrix} \cos\lambda & 0 & \sin\lambda \\ 0 & 1 & 0 \\ -\sin\lambda & 0 & \cos\lambda \end{bmatrix} - \begin{bmatrix} \cos\theta_1 & \sin\theta_1 & 0 \\ -\sin\theta_1 & \cos\theta_1 & 0 \\ 0 & 0 & 1 \end{bmatrix} \begin{bmatrix} X \\ Y \\ Z \end{bmatrix}$$

This product is solved according to the series of equations:

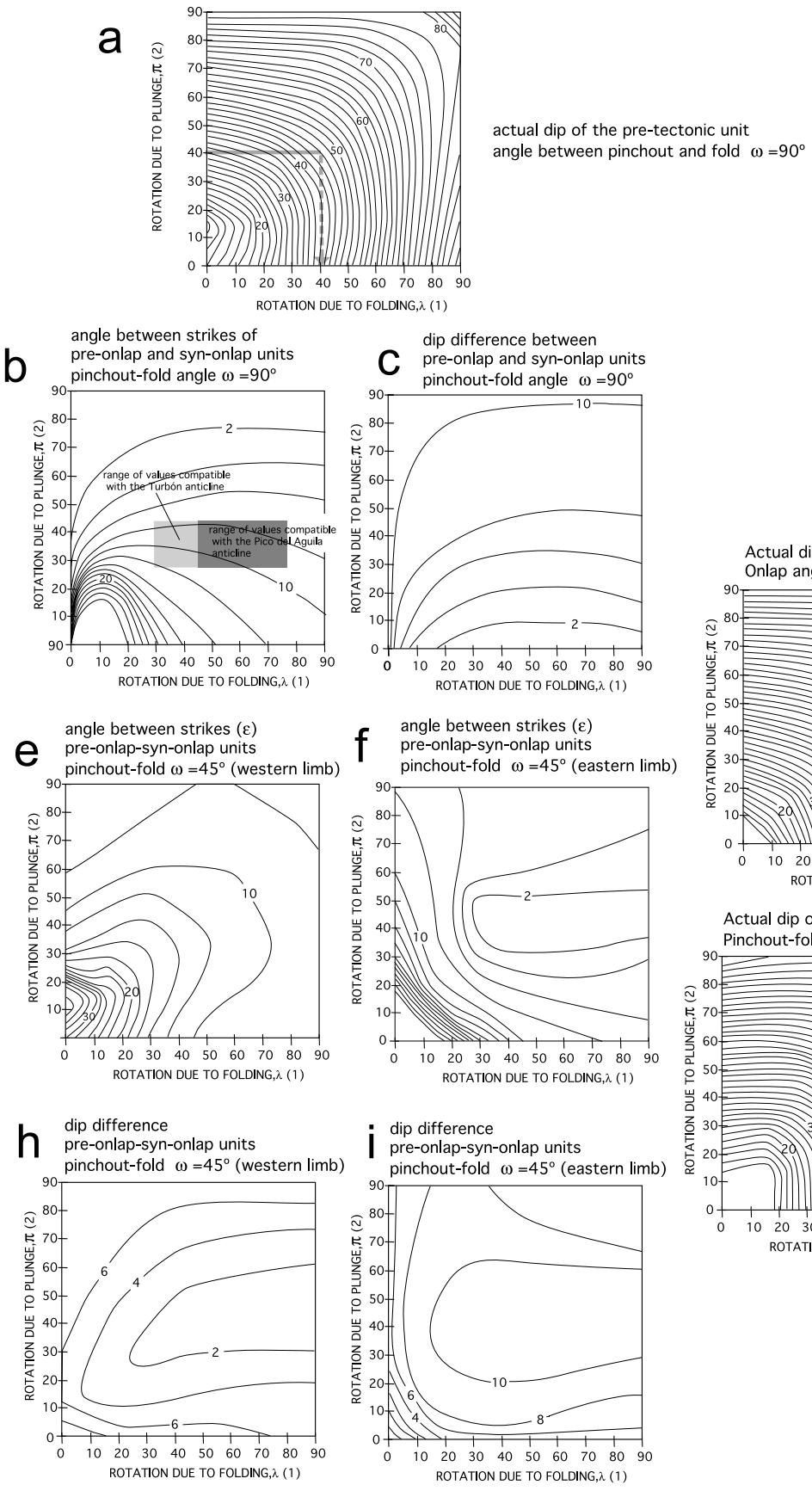
a
actual dip of the pre-tectonic unit
angle between pinchout and fold ω =90°
b
angle between strikes of
pre-onlap and syn-onlap units
pinchout-fold angle ω =90°
range of values compatible with the Turbón anticline
range of values compatible with the Pico del Aguila anticline
c
dip difference between
pre-onlap and syn-onlap units
pinchout-fold angle ω =90°
d
Actual dip of syn-onlap unit
Onlap angle (Ω) 10°
e
angle between strikes (ε)
pre-onlap-syn-onlap units
pinchout-fold ω =45° (western limb)
f
angle between strikes (ε)
pre-onlap-syn-onlap units
pinchout-fold ω =45° (eastern limb)
g
Actual dip of pre-onlap unit
Pinchout-fold angle ω =45°
h
dip difference
pre-onlap-syn-onlap units
pinchout-fold ω =45° (western limb)
i
dip difference
pre-onlap-syn-onlap units
pinchout-fold ω =45° (eastern limb)
ROTATION DUE TO PLUNGE,π (2)
ROTATION DUE TO FOLDING,λ (1)

$$X' = X(\sin^2\theta_1 + \cos^2\theta_1\cos\lambda) + Y(\sin\theta_1\cos\theta_1\cos\lambda - \cos\theta_1\sin\theta_1) + Z(\cos\theta_1\sin\lambda)$$

$$Y' = X(\cos\theta_1\sin\theta\cos\lambda - \sin\theta_1\cos\theta_1) + Y(\sin^2\theta_1\cos\lambda + \cos\lambda + \cos^2\theta_1) + Z(\sin\theta_1\sin\lambda)$$

$$Z' = X(-\cos\theta_1\sin\lambda) + Y(-\sin\theta_1\sin\lambda) + Z(\cos\lambda)$$

Coordinates of the vector after rotation about the second axis (X'', Y'', Z'') can be calculated in the same way, considering them as the parameters of the transform matrix, the azimuth of the second rotation axis and the amount of rotation about this axis (ψ_2 is the azimuth of the second rotation axis, $\theta_2 = 90 + \psi_2$ is the azimuth perpendicular to this axis and π is the angle of rotation about this second axis). The matrix product is then:

$$\begin{bmatrix} X'' \\ Y'' \\ Z'' \end{bmatrix} = \begin{bmatrix} \cos\theta_2 & -\sin\theta_2 & 0 \\ \sin\theta_2 & \cos\theta_2 & 0 \\ 0 & 0 & 1 \end{bmatrix} \begin{bmatrix} \cos\pi & 0 & \sin\pi \\ 0 & 1 & 0 \\ -\sin\pi & 0 & \cos\pi \end{bmatrix} - \begin{bmatrix} \cos\theta_2 & \sin\theta_2 & 0 \\ -\sin\theta_2 & \cos\theta_2 & 0 \\ 0 & 0 & 1 \end{bmatrix} \begin{bmatrix} X' \\ Y' \\ Z' \end{bmatrix}$$

which can be solved in an identical way. The strike and dip of the rotated plane can be obtained from the coordinates of the vector:

$$\delta'' = \tan^{-1}\left(\frac{X''}{Y''}\right) \pm 360°, \quad \beta'' = \tan^{-1}\left(\frac{Z''}{\sqrt{X''^2 + Y''^2}}\right)$$

It must be taken into account that, when applying these equations, rotations are always counterclockwise looking from the centre of the projection towards the azimuth of the rotation axis.

In the calculations made, the parameter related with rotation due to folding (λ) is not the present-day dip of beds, but the amount of the first rotation. To obtain the rotation angle from the actual dip of beds in the fold limb some conversions must be made, separately in the pre- and syn-onlap sequences. These conversions are also different for different angles between the pinchout lines and the axial trace of folds (ω) (Fig. 4a, d and g). These values can be directly obtained from the co-ordinates of the vectors (X'', Y'', Z'') representing the planes and comparing the dip values for the planes with the amount of rotation about each of the two axes λ and π.

The relationships obtained indicate that the angle between strikes of the pre- and syn-onlap sequences (ε) can reach extreme values of 40°, in the cases of very gentle folding and low plunge. Even greater values could be obtained for rotation angles lower than 10°, but in these cases bedding can be considered as nearly horizontal, and the angle between strikes is not relevant. The angle ε becomes progressively smaller as the plunge of fold increases, and more rapidly with increasing rotation due to folding (Fig. 4b). For ω values different from 90°, ε is different in both limbs of the fold, being generally higher (for equal rotation values) in the western limb than in the eastern limb, under the modelled conditions.

Differences in dip between the pre- and syn-onlap series are regular for $\omega = 90°$, increasing as the rotation associated with plunge increases. For $\omega = 45°$ the pattern of variation for dip differences is considerably different in both limbs of the fold, with a minimum and a maximum in the western and eastern limb, respectively, for values of rotation associated with plunge of about 45°.

2.3. Cartographic patterns

From the diagrams shown in Fig. 4, forward modelling of cartographic patterns reproducing the imposed conditions, can be done. To show the possibilities of using these diagrams we constructed several hypothetical geological maps, completing the qualitative approach shown previously (Fig. 2), with different values of the initial parameters (Fig. 2e, f, i and j). In two of them (Fig. 2e and f) we exemplify symmetric anticlines with box-fold geometry. The fold axis is perpendicular to the pinchout line ($\omega = 90$), the onlap angle is $\Omega = 10°$, the rotation values due to fold plunge are $\pi = 30°$ and $\pi = 20°$, respectively, and

Fig. 4. Diagrams allowing the difference in strike and dip between the syn- and pre-onlap beds to be obtained from the angles of limb rotation λ (folding, horizontal axis in diagrams), and rotation associated with plunge of folds, π (vertical axis in diagrams). The intersection between pre- and syn-onlap beds (pinchout line) is perpendicular to the trend of the axis of folding ($\omega = 90°$) in diagrams (a)–(c), and oblique ($\omega = 45°$) for diagrams (e)–(j). The onlap angle (Ω) is 10° in all cases. Contour interval is 2° for all diagrams. (a) Conversion diagram to obtain the angle of rotation of the pre-onlap series associated with fold (in abscise axis in all diagrams), from the final fold limb and tilting. The way to determine the amount of rotation due to folding, from the plunge angle and the final dip of beds is indicated by the arrow. (b) Contours showing the angle between strikes of pre-onlap beds and syn-onlap beds. Shaded rectangles indicate the average values for the Turbón-Egea and the Pico del Aguila anticlines. (c) Contours showing the dip difference between syn- and pre-onlap beds. (d) Final dip of beds of the syn-onlap series, considered as originally horizontal, after limb rotation and plunging for an onlap angle of 10°. This diagram can be applied to all cases, whatever the angle (ω) of fold axis with the pinchout line. The way to determine the amount of rotation due to folding is the same as for diagram (a). (e) Contours showing the angle between the strike of pre- and syn-onlap beds, in the western limb of the fold, for an onlap angle of 10° and an angle of 45° between the fold axis and the pinchout line. (f) Idem to (e) in the eastern fold limb. (g) Final dip of beds of the pre-onlap series after limb rotation and tilting (onlap 10°) for an angle of 45° between the pinchout line of the syn-onlap sequence and the fold axis. (h) Contours showing the dip difference between syn- and pre-onlap beds in the western limb of the fold. (i) Idem to (h) in the eastern limb of the fold.

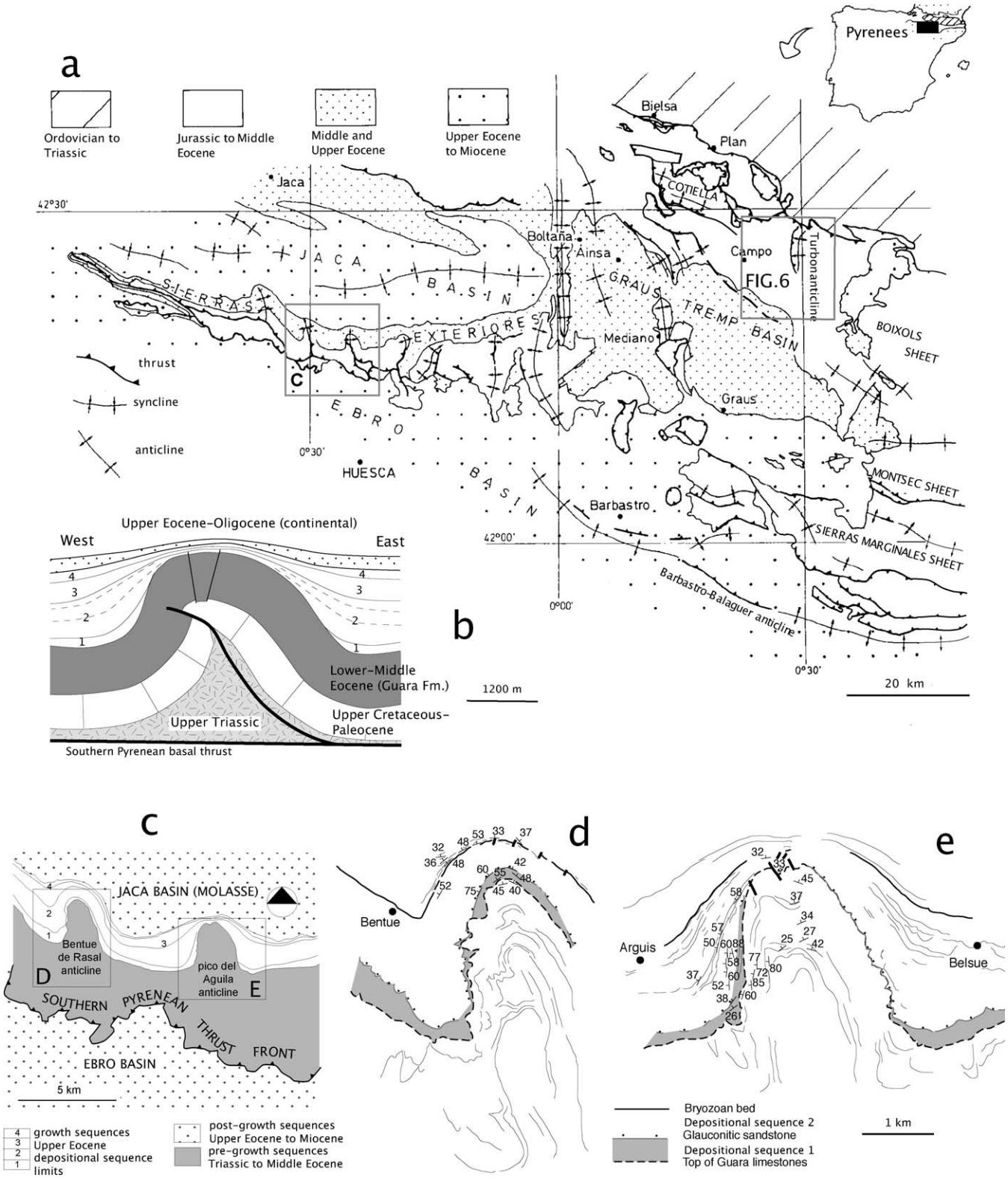

Fig. 5. (a) Geological sketch of the Southern Pyrenees showing the two areas with N–S folds discussed in this paper and the location of sketch of (c). Modified from Martínez-Peña and Casas-Sainz (2003). (b) Cross-section of the Pico del Aguila anticline from dip data and taking into account the cartographic pattern of the pre-growth and growth units (dip data from Poblet and Hardy (1995), Pueyo (2000) and Montes-Santiago (2002)). It is important to remark that, strictly, Wilson's (1967) method cannot be used to reconstruct the fold, because of the uneven topography (cuestas and hog-backs in the Eocene limestones, with nearly horizontal envelopes) and the complicated relationships between topography and outcrops of units with strong competence contrasts. The application of this method would lead to important errors, such as the exaggeration of the dips of strata in the western limb of the anticline, which show maximum averaged values of 70–80° according to direct measurements (Poblet and Hardy, 1995). (c) Geological sketch of the Pico del Aguila and Bentué de Rasal anticlines (Sierras

rotation in fold limbs are $\lambda = 60°$ and $\lambda = 20°$, respectively. Under the conditions imposed in the anticline shown in Fig. 2e the dip of the pre-onlap beds is 58° in the fold limbs and 30° in the hinge zone. The dip of the syn-onlap sequence is 64° in limbs and the calculated angle between the strikes of the pre-onlap and syn-onlap sequences is 8°. In the anticline shown in Fig. 2f the angle between strikes of the pre- and syn-onlap sequences is higher. In both cases, the obtained cartographic pattern is similar to a sequence of growth strata associated with the anticline and apparently thinning in its hinge zones.

In the third quantitative model presented (Fig. 2i) the axis of folding is considered as oblique to the pinchout line ($\omega = 45°$), and the axis direction of the second rotation is perpendicular to the first rotation, in such a way that the pinchout line bisects the 90° angle between the rotation axes. The cartographic pattern of this geometry is considerably different from the first model, with the angle between the strikes of pre- and syn-onlap beds more pronounced in the western limb of the anticline with respect to its eastern limb. Since the pinchout line is oblique to the second fold axis the syn-onlap sequence gradually disappears toward the east.

The fourth quantitative cartographic pattern (Fig. 2j) represents the effect of two subsequent rotations about two non-perpendicular axes (forming an angle of 45°), with the pinchout line parallel to the second rotation axis and oblique to the first rotation axis ($\omega = 45°$). This situation is not represented in diagrams of Fig. 4 but angles between the strikes of the pre- and syn-onlap sequences can be obtained changing the parameters of the equations shown in Section 2.2. This pattern may reproduce a geological situation in which the first fold is transported over an oblique ramp, parallel to the former basin margin. The result indicates a larger angle between the beds of the syn- and pre-onlap sequences in the western limb versus a lower unconformity angle at the eastern limb (as in Fig. 5d).

3. Comparison with natural examples of 'syn-sedimentary' folds

To test the implications of the theoretical models developed, we have focused the application of the geometrical models presented in several folds from two areas in the southern Pyrenees. The southern Pyrenees are characterised by the good preservation of the syn-tectonic sedimentary sequences deposited during the Eocene–Oligocene, Pyrenean compression. Geometrical relationships of growth strata can be assessed from map view, good exposures, and, in some areas, seismic reflection profiles (Ford et al., 1997; Suppe et al., 1997).

The Pico del Aguila and Bentué de Rasal anticlines are located in the Sierras Exteriores Aragonesas (Fig. 5). The axis of the Pico del Aguila plunges at 29° towards 353° and the Bentué de Rasal anticline plunges at 40° towards 010°, according to Pueyo (2000) and Pueyo et al. (2002). Therefore, they are perpendicular to oblique to the main E–W to NW–SE strike of the frontal Pyrenean thrust in this area. The axial traces of both folds can be followed for 2 km. Their geometry can be considered as combined kink-type and flexural folds, with angular to rounded hinges and rectilinear to curved limbs (see cross-section in Fig. 5b and also in Poblet and Hardy (1995) and Poblet et al. (1997)). The southern Pyrenean thrust underlies the N–S folds in this area. Its geometry can be characterised as a hanging wall flat over a footwall ramp with an average dip of 30° (Millán, 1996; Pueyo, 2000). The movement along this ramp is responsible for the 30° plunge of N–S fold axes in this area. The present-day dips of the pre-growth sequence in the limbs of the two anticlines are between 30 and 80° in the central outcropping part of the folds (Fig. 5d and e; see also Millán, 1996; Poblet and Hardy, 1995). The Middle–Late Eocene strata (mainly marls from the Arguis–Pamplona Fm.) are considered the growth series (see Poblet and Hardy, 1995; Pueyo et al., 2002). From photogeological studies (see Fig. 5d and e) it can be assessed that some of the depositional sequences of this series thin northwards (with a maximum 1:6 thickness ratio in the Pico del Aguila anticline) along the limbs of both anticlines, although no clear lapouts can be distinguished. Moreover, the stratigraphic contacts are masked by the existence of small-scale faults between the pre- and the syn-growth sequences (see Fig. 5d and e). The angles between the strike of beds of the pre- (Guara Fm.) and syn-growth (depositional sequences 2 and 3 of Arguis–Pamplona Fm.) series vary between 20° in the western limb and 7° in the eastern limb in the Pico del Aguila anticline ($\varepsilon = 7–15°$). In the first depositional sequence there are no significant strike changes with respect to the pre-growth sequence. In the Bentué de Rasal anticline the average angles between the pre- and syn-onlap (depositional sequence 3 of Arguis–Pamplona Fm.; see Fig. 5d) sequences are higher (Millán et al., 1994; Montes-Santiago, 2002), reaching 30° in its western limb.

Can the Bentué de Rasal and Pico del Aguila anticlines be interpreted as younger than the Arguis–Pamplona Fm. according to the models presented in previous sections? Examining the angular relationships available from outcrop observations, the outcrop pattern of the growth sequence in the Pico del Aguila anticline is consistent with a 50–70°

Exteriores, southern Pyrenees) showing the geometry of the 'syn-tectonic' sequence. Redrawn from Millán et al. (1994), Pueyo (2000) and Montes-Santiago (2002). The locations of photogeological sketches of (d) and (e) are shown. (d) Photogeological sketch of the Bentué de Rasal anticline. (e) Photogeological sketch of the Pico del Aguila anticline with dip data obtained in this work.

rotation in the N–S fold limb followed by a 30° rotation according to a perpendicular axis, with a pinchout line perpendicular to the first fold axis (see Fig. 4). Sediments of the first sequences within the Arguis–Pamplona Fm. have been classically considered as slope marls (Puigdefàbregas, 1975) and, therefore, the basal contact of this unit on the pre-growth limestones could be a downlap. Sedimentological data support the hypothesis of a downlap geometry of the first sedimentary sequence within the Arguis–Pamplona Fm., consisting of pro-delta or platform marls, prograding northwards (Puigdefàbregas, 1975; Castelltort et al., 2000; Montes-Santiago, 2002). From the detailed photogeological sketch (Fig. 5e) it can be remarked that the pinchout of the lapout is oblique with respect to the fold axis. The subsequent sedimentary sequences within the Arguis Fm. evolve to deltaic systems or siliciclastic platforms with westward polarity. The cartographic pattern resulting from the geometric array of the first sedimentary sequence of the Arguis Fm. would be very similar to Fig. 2e. If this was the case, some of the deformation associated with the Pico del Aguila anticline could post-date deposition of the first sedimentary sequence and could be interpreted as partly contemporary with the movement of the frontal ramp of the southern Pyrenean thrust. In the Bentué de Rasal anticline the first two units show no significant thickness changes toward the hinge of the anticline. Nevertheless, a reduction in thickness is observed for the first depositional sequence in its western limb (Fig. 5d). The third depositional sequence is thinned in the hinge zone, although no lapout against the lower sequences of the Arguis Fm. can be clearly distinguished. When interpreted according to the model presented in this work, the Bentué de Rasal anticline is consistent with a 30–45° angle between the fold axis responsible for the first rotation and the pinchout line (cartographic pattern similar to Fig. 2j). According to this model, the fold axis responsible for the second rotation must be parallel to the trend of the pinchout line. To fit with the proposed model the pinchout lines of the Arguis–Pamplona Fm. should also be parallel to the present-day mapped trace of the southern Pyrenean thrust (Fig. 5), responsible for the second rotation. The compressional structure so obtained would then be conditioned by the previous geometry of sedimentary units, as occurs in analogue experiments and other natural examples (Barrier et al., 2002). Nevertheless, as will be discussed later on, to corroborate these hypotheses explaining the present-day outcrop pattern of these folds, a vertical section would be necessary. Unfortunately, up-to-date existing seismic reflection profiles in the southern Pyrenees do not provide a reliable picture of the shallow subsurface near these N–S folds.

The N–S-trending Turbón and Egea anticlines are located in the hanging wall of the Cotiella-Bóixols thrust, near the Axial zone of the Pyrenees (see Figs. 5 and 6). They show a southward plunge and the limb dips between vertical and 30°. These folds are developed on Cretaceous marine rocks. The pre-growth sequence consists of platform limestones, and the syn-growth sequence, thinning in the hinge zone of anticlines according to geological maps (Figs. 6 and 7), consists of turbidites (Simó, 1985). This turbiditic sequence (Vallcarga Fm.) reduces in thickness toward the South, passing to platform sediments in the Montsec unit (Simó, 1985). The average dip of limbs ranges between 30 and 50°, although they reach 90° in some outcrops. Structures show a westward vergence, with a better defined eastern limb of anticlines in seismic sections (Figs. 6 and 7a). The seismic reflection profiles parallel and perpendicular to the fold axes (Fig. 7b) indicate an average plunge of folds of about 30°, reaching 90° at surface, in the hinge zone of the Turbón anticline.

The most remarkable feature that can be observed in the seismic sections in the Turbón area is the increase in thickness of the Cretaceous marls and turbidites (lower part of the Vallcarga Fm.) toward the hinge zone of the anticlines (Fig. 7a). This geometry is in contrast with the cartographic pattern, showing a thinning of the same units in the hinge area. This contradiction can be explained according to our geometrical models (see Fig. 1), and considering a southward reduction in thickness, consistent with basin reconstruction in this area (Simó, 1985; Martínez-Peña and Casas-Sainz, 2003). Conversely, the upper part of the Vallcarga Fm. can be interpreted to be contemporary with the Turbón and Egea anticlines, since its thinning toward the hinge zone can be observed both in map view and seismic sections. The Turbón-Egea fold system can then be interpreted as the result of N–S oriented folding, partly coeval with Late Cretaceous turbiditic deposition in this area, although its formation took place probably later than considered up to date (upper part of the Vallcarga Fm.).

4. Discussion and conclusions

The geometrical analysis shown in this work indicates that similar cartographic patterns can be obtained either by folding contemporary with deposition of a syn-tectonic sedimentary unit, or by folding of a previous geometry, linked to basin margins (onlap). In the latter case, the thinning of the pre-folding series toward the basin margin gives a false appearance of syn-onlap sediments associated with folds perpendicular to this basin margin. Downlap geometries may also give similar cartographic patterns when folded in two oblique or mutually perpendicular directions. Apparent onlap geometries at the base of the growth sequences are especially ambiguous, since they can form by the two mechanisms (syn- or post-sedimentary folding). The modelling described here has important implications in the interpretation of the age of folds.

In spite of the difficulty of determining the origin of unconformities related to folds, there are some criteria, derived from the theoretical models presented and the analysis of the field examples, that can be used to distinguish between the two possible relationships, even in

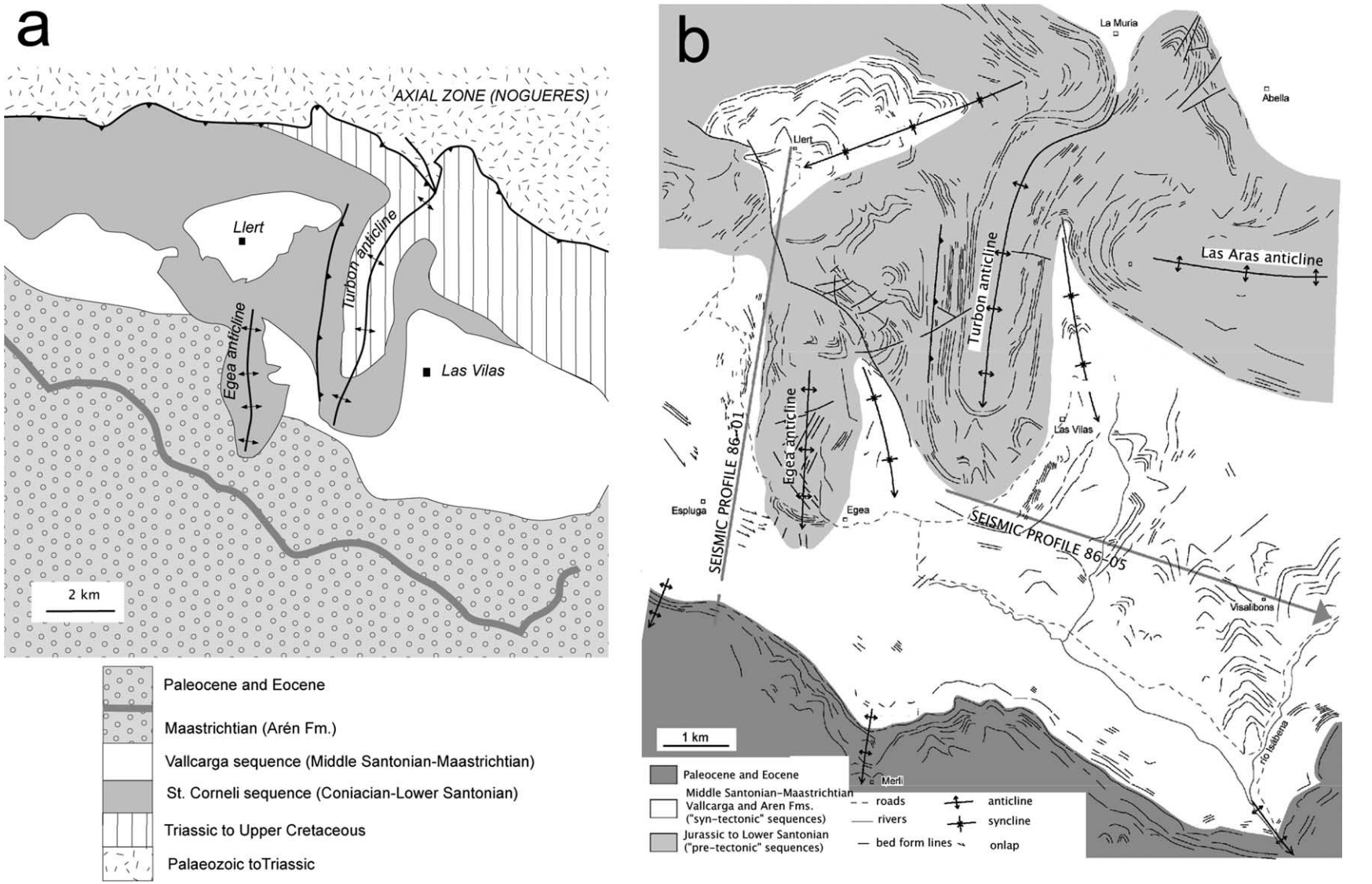

Fig. 6. (a) Geological map of the Turbón-Egea anticlines area (modified from Simó, 1985). (b) Photogeological sketch drawn from aerial photographs, with field data of the same area. The locations of seismic sections of Fig. 7 are shown.

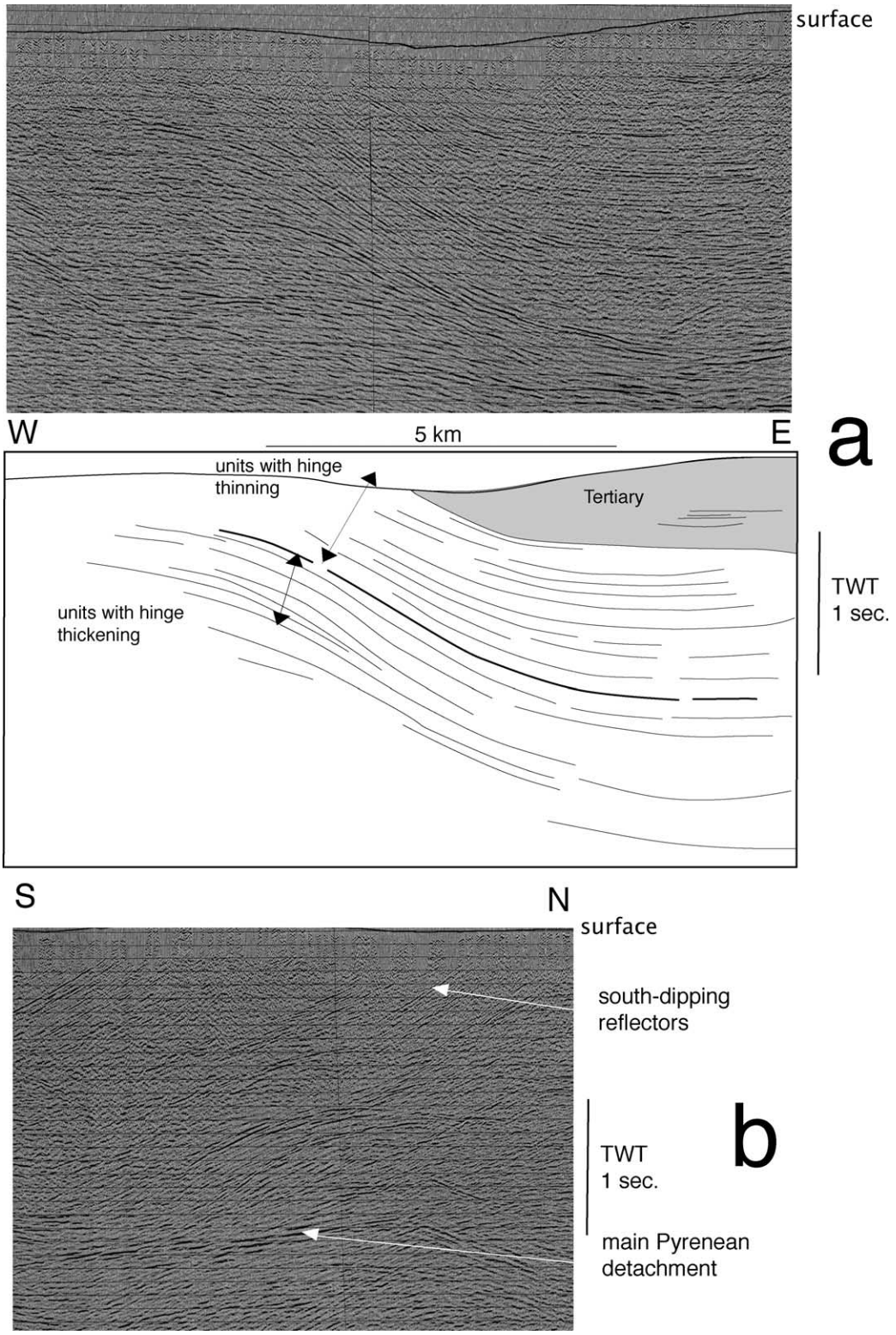

Fig. 7. Seismic reflection profiles across the eastern part of the Turbón-Egea fold system. See location in Fig. 6b. (a) Seismic profile SP 86-05. (b) Seismic profile SP 86-01. Source: Repsol-exploración.

the absence of an independent data source (e.g. seismic sections parallel and perpendicular to the fold axis):

– When the onlap is previous to folding (model shown in Fig. 1), in the modelled conditions, the dips of strata of the syn-onlap sequence are systematically steeper than those of the pre-onlap sequence by a few degrees (see Fig. 2e, f, i and j).

This relationship can be different in the case of syn-tectonic sequences coeval with folding. However, this criterion is not easy to apply when the critical accuracy in measuring bed orientation cannot be achieved (e.g. massive or nodulose limestones).

– When the thickness-changing units are related to the uplift of an individual fold there must be a consistent relationship between the lapouts and the limbs of the folds. This criterion can be applied to sequence 1 of the Arguis–Pamplona Fm. in the Pico del Aguila anticline and sequences 1 and 3 in the Bentué de Rasal anticline to conclude that there is probably no relationship between the uplift of the folds and the deposition of these units.
– When the syn-growth, variable-thickness series is actually syn-tectonic, coeval with the fold, some geometrical criteria can be used, though they are different when applied to rotating (i.e. flexural-slip folds) and non-rotating (i.e. kink-type folds) limbs: (i) in the case of non-rotating limbs (kink-type folds) the existence of an angular unconformity (formed when the uplift/sedimentation ratio is higher than 1), can be used to define the coeval relationship between fold and sediments; (ii) when the fold is formed by limb rotation the gradual change in dip and internal unconformities within the growth strata are the only criteria to define this relationship. Offlap, or toplap geometries within the syn-onlap series (normally associated with intra-basinal unconformities) are less ambiguous features or, at least, they cannot form under the conditions imposed in the previous onlap models.

In two of the cases studied (Pico del Aguila and Bentué de Rasal anticlines), the use of these criteria is limited by the outcrop conditions, which do not allow a clear identification (either in the field or from aerial photographs) of the features of the unconformities within growth strata. Although new research on this subject was carried out, carefully measuring the strike and dip of beds of the growth sequence (Fig. 5d and e), the results obtained do not give any conclusive indications about the age of folds. However, the detailed mapping (Fig. 5d and e) allows the determination that the lapouts of the first depositional sequence of the Arguis–Pamplona Fm. are not related to the Pico del Aguila uplift. The same criterion can be applied to the third depositional sequence of the Bentué de Rasal anticline, since the progressive unconformity (as defined by Riba (1976)) can only be distinguished in the western limb of the fold. The criterion using dips of the pre- and syn-growth sequences is consistent with previous works (Millán et al., 1994) in the Bentué de Rasal anticline: the first sequences of the Arguis–Pamplona Fm. show higher dips than the Guara Fm., indicating that the Arguis–Pamplona marls are probably lapping out towards the North on the Guara limestones and the fold post-dates these units. We can finally conclude that the Pico del Aguila anticline was probably coeval with the middle part of the Arguis Fm., as indicated by a probable thinning of beds within this unit. The Bentué de Rasal anticline is probably coeval with the upper part of the Arguis Fm., although the criteria are weaker than in the former case, especially because of the difficulty of determining the trend of the pinchout line of the growth strata. The folds in the Turbón-Egea system are better constrained because of the good-quality seismic profiles in two perpendicular directions.

The analysis shown in this work can be also be applied to two-dimensional sections given by seismic reflection profiles where there is not a complementary control from geological maps (or serial marine profiles). In this case, the vertical section can behave as the horizontal section in our analysis. Some apparent geometrical paradoxes appearing in seismic sections, such as sequences thickening in the hinge zone of anticlines, could be explained by the models shown in this paper (Sikder and Alam, 2003, their fig. 4).

In marine sediments the presence of lapouts related to limits of depositional sequences or with maximum flooding surfaces is relatively common. The geometrical arrangements described in this work may be more frequent than recognised up to now in the geological literature. From the geometrical models shown in this work it can be seen that tectonic analysis based on the geometry of growth strata must always be accompanied, if possible, by a 3-D study. Both seismic or topographic sections and geological maps are needed to define the geometrical relationships between pre- and syn-tectonic units. Serial parallel seismic sections can also help to constrain the growth strata associated with structures. The reliability of the relationships established lies on the independence of the two sources from which maps and cross-sections are obtained (i.e. cross-sections derived only from geological maps may not be necessarily true).

Acknowledgements

The authors are very grateful to Mary Ford, Fabrizio Storti and Thomas Blenkinsop for their helpful reviews. This work was supported by project BTE-2002-04168 of the Spanish Ministry of Science and a FPI grant to Ruth Soto. The authors are also grateful to Repsol-exploración for allowing to use and copy the seismic reflection profiles shown in this paper.

References

Barrier, L., Nalpas, T., Gapais, D., Proust, J.N., Casas, A., Bourquin, S.,

2002. Influence of syntectonic sedimentation on thrust geometry. Field examples from the Iberian Chain (Spain) and analogue modelling. Sedimentary Geology 146, 91–104.

Castelltort, S., Guillocheau, F., Nalpas, T., Rouby, D., Robin, C., Urreiztieta, M., Coutand, I., 2000. Tectonically induced distortion of stratigraphic cycles. Example of the Arguis anticline in the South Central Pyrenees (Spain). Geotemas 2, 55–58.

Cortés, A.L., Liesa, A.R., Soria, A.R., Meléndez, A., 1999. Role of extensional structures on the location of folds and thrusts during tectonic inversion (northern Iberian Chain, Spain). Geodinamica Acta 12 (2), 113–132.

Ford, M., Williams, E.A., Artoni, A., Vergés, J., Hardy, S., 1997. Progressive evolution of a fault-related fold pair from growth strata geometries, Sant Llorenç de Morunys, SE Pyrenees. Journal of Structural Geology 19 (3–4), 413–441.

Martínez-Peña, M.B., Casas-Sainz, A.M., 2003. Cretaceous–Tertiary tectonic inversion at the Cotiella Nappe (Southern Pyrenees, Spain). International Journal of Earth Sciences 92, 99–113.

Millán, H., 1996. Estructura y cinemática del frente de cabalgamiento surpirenaico en las Sierras Exteriores Aragonesas. Unpublished PhD Thesis, University of Zaragoza, 330pp.

Millán, H., Aurell, M., Meléndez, A., 1994. Synchronous detachment folds and coeval sedimentation in the Prepyrenean External Sierras (Spain): a case study for a tectonic origin of sequences and system tracts. Sedimentology 41, 1001–1024.

Montes-Santiago, M.J., 2002. Estratigrafía del Eoceno-Oligoceno de la Cuenca de Jaca (sinclinorio del Guarga). Unpublished PhD Thesis, University of Barcelona.

Poblet, J., Hardy, S., 1995. Reverse modelling of detachment folds; application to the Pico del Aguila anticline in the South Central Pyrenees (Spain). Journal of Structural Geology 17 (12), 1707–1724.

Poblet, J., McClay, K., Storti, F., Muñoz, J.A., 1997. Geometries of syntectonic sediments associated with single-layer detachment folds. Journal of Structural Geology 19, 369–381.

Pueyo, E., 2000. Rotaciones paleomagnéticas en sistemas de cabalgamientos: Tipos, causas, significados y aplicaciones (Ejemplos de las Sierras Extriores y de la Cuenca de Jaca, Pirineo Aragonés). Unpublished PhD Thesis, University of Zaragoza, 299pp.

Pueyo, E.L., Millán, H., Pocovi, A., 2002. Rotation velocity of a thrust: a paleomagnetic study in the External Sierras (Southern Pyrenees). Sedimentary Geology 146, 191–208.

Puigdefàbregas, C., 1975. La sedimentación molásica en la Cuenca de Jaca, Monografías del Instituto de Estudios Pirenaicos 104, 108pp.

Ramsay, J.G., 1967. Folding and Fracturing of Rocks. McGraw-Hill, New York. 560pp.

Riba, O., 1976. Syntectonic unconformities in the Alto Cardener, Spanish Pyrenees: a genetic interpretation. Sedimentary Geology 15, 213–233.

Sikder, A.M., Alam, M.M., 2003. 2-D modelling of the anticlinal structures and structural development of the eastern fold belt of the Bengal Basin, Bangladesh. Sedimentary Geology 155, 209–226.

Simó, A., 1985. Secuencias deposicionales del Cretácico superior de la Unidad del Montsec (Pirineo Central). Unpublished PhD Thesis, University of Barcelona, 326pp.

Spiegel, M.R., 1998. Schaum's Mathematical Handbook of Formulas and Tables. McGraw-Hill, New York. 278pp.

Storti, F., Poblet, J., 1997. Growth stratal architectures associated with décollement folds and fault-propagation folds: inferences on fold kinematics. Tectonophysics 282, 353–373.

Suppe, J., Chou, G.T., Hook, S.C., 1992. Rates of folding and faulting determined from growth strata. In: McClay, K.R. (Ed.), Thrust Tectonics. Chapman & Hall, London, pp. 105–121.

Suppe, J., Sábat, F., Muñoz, J.A., Poblet, J., Roca, E., Vergés, J., 1997. Bed-by-bed fold growth by kink-band migration: Sant Llorenç de Morunys, eastern Pyrenees. Journal of Structural Geology 19 (3–4), 443–461.

Van Wagoner, J.C., Posamentier, H.W., Mitchum, R.M., Vail, P.R., Sarg, J.F., Loutit, T.S., Hardenbol, J., 1988. An overview of the fundamentals of sequence stratigraphy and key definitions. In: Wilgus, C.K., Hastings, B.S., Kendall, C.G.St.C., Posamentier, H.W., Ross, C.A., Van Wagoner, J.C. (Eds.), Sea-Level Changes: an Integrated Approach Soc. Econ. Paleontol. Mineral. Spec. Publ. 42, pp. 39–45.

Vergés, J., Marzo, M., Muñoz, J.A., 2002. Growth strata in foreland settings. Sedimentary Geology 146, 1–10.

Wilson, G., 1967. The geometry of cylindrical and conical folds. Proceedings of the Geological Association 78, 179–210.